

EAD: Elastic-Net Attacks to Deep Neural Networks via Adversarial Examples

Pin-Yu Chen^{*,1}, Yash Sharma^{*,1}, Huan Zhang^{1,2}, Jinfeng Yi¹, Cho-Jui Hsieh²

¹AI Foundations Group, IBM T. J. Watson Research Center, Yorktown Heights, NY 10598, USA

²University of California, Davis, Davis, CA 95616, USA

pin-yu.chen@ibm.com, ysharma1126@gmail.com, ecezhang@ucdavis.edu, jinfengyi@us.ibm.com, chohsieh@ucdavis.edu

Abstract

Recent studies have highlighted the vulnerability of deep neural networks (DNNs) to adversarial examples - a visually indistinguishable adversarial image can easily be crafted to cause a well-trained model to misclassify. Existing methods for crafting adversarial examples are based on L_2 and L_∞ distortion metrics. However, despite the fact that L_1 distortion accounts for the total variation and encourages sparsity in the perturbation, little has been developed for crafting L_1 -based adversarial examples.

In this paper, we formulate the process of attacking DNNs via adversarial examples as an elastic-net regularized optimization problem. Our elastic-net attacks to DNNs (EAD) feature L_1 -oriented adversarial examples and include the state-of-the-art L_2 attack as a special case. Experimental results on MNIST, CIFAR10 and ImageNet show that EAD can yield a distinct set of adversarial examples and attains similar attack performance to the state-of-the-art methods in different attack scenarios. More importantly, EAD leads to improved attack transferability and complements adversarial training for DNNs, suggesting novel insights on leveraging L_1 distortion in adversarial learning and security implications for DNNs.

Introduction

Deep neural networks (DNNs) achieve state-of-the-art performance in various tasks in machine learning and artificial intelligence, such as image classification, speech recognition, machine translation and game-playing. Despite their effectiveness, recent studies have illustrated the vulnerability of DNNs to adversarial examples (Szegedy et al. 2013; Goodfellow, Shlens, and Szegedy 2015). For instance, a carefully designed perturbation to an image can lead a well-trained DNN to misclassify. Even worse, effective adversarial examples can also be made virtually indistinguishable to human perception. For example, Figure 1 shows three adversarial examples of an ostrich image crafted by our algorithm, which are classified as “safe”, “shoe shop” and “vacuum” by the Inception-v3 model (Szegedy et al. 2016), a state-of-the-art image classification model.

The lack of robustness exhibited by DNNs to adversarial examples has raised serious concerns for security-critical applications, including traffic sign identification and malware detection, among others. Moreover, moving beyond



Figure 1: Visual illustration of adversarial examples crafted by EAD (Algorithm 1). The original example is an ostrich image selected from the ImageNet dataset (Figure 1 (a)). The adversarial examples in Figure 1 (b) are classified as the target class labels by the Inception-v3 model.

the digital space, researchers have shown that these adversarial examples are still effective in the physical world at fooling DNNs (Kurakin, Goodfellow, and Bengio 2016; Evtimov et al. 2017). Due to the robustness and security implications, the means of crafting adversarial examples are called *attacks* to DNNs. In particular, *targeted attacks* aim to craft adversarial examples that are misclassified as specific target classes, and *untargeted attacks* aim to craft adversarial examples that are not classified as the original class. *Transfer attacks* aim to craft adversarial examples that are transferable from one DNN model to another. In addition to evaluating the robustness of DNNs, adversarial examples can be used to train a robust model that is resilient to adversarial perturbations, known as *adversarial training* (Madry et al. 2017). They have also been used in interpreting DNNs (Koh and Liang 2017; Dong et al. 2017).

Throughout this paper, we use adversarial examples to attack image classifiers based on deep convolutional neural networks. The rationale behind crafting effective adversarial examples lies in manipulating the prediction results while ensuring similarity to the original image. Specifically, in the literature the similarity between original and adversarial examples has been measured by different distortion metrics. One commonly used distortion metric is the L_q norm, where $\|\mathbf{x}\|_q = (\sum_{i=1}^p |\mathbf{x}_i|^q)^{1/q}$ denotes the L_q norm of a p -dimensional vector $\mathbf{x} = [\mathbf{x}_1, \dots, \mathbf{x}_p]$ for any $q \geq 1$. In particular, when crafting adversarial examples, the L_∞ distortion metric is used to evaluate the maximum variation in pixel value changes (Goodfellow, Shlens, and Szegedy

*Pin-Yu Chen and Yash Sharma contribute equally to this work.

2015), while the L_2 distortion metric is used to improve the visual quality (Carlini and Wagner 2017b). However, despite the fact that the L_1 norm is widely used in problems related to image denoising and restoration (Fu et al. 2006), as well as sparse recovery (Candès and Wakin 2008), L_1 -based adversarial examples have not been rigorously explored. In the context of adversarial examples, L_1 distortion accounts for the total variation in the perturbation and serves as a popular convex surrogate function of the L_0 metric, which measures the number of modified pixels (i.e., sparsity) by the perturbation. To bridge this gap, we propose an attack algorithm based on elastic-net regularization, which we call **elastic-net attacks to DNNs (EAD)**. Elastic-net regularization is a linear mixture of L_1 and L_2 penalty functions, and it has been a standard tool for high-dimensional feature selection problems (Zou and Hastie 2005). In the context of attacking DNNs, EAD generalizes the state-of-the-art attack proposed in (Carlini and Wagner 2017b) based on L_2 distortion, and is able to craft L_1 -oriented adversarial examples that are fundamentally different from existing attack methods.

To explore the utility of L_1 -based adversarial examples crafted by EAD, we conduct extensive experiments on MNIST, CIFAR10 and ImageNet in different attack scenarios. Compared to the state-of-the-art L_2 and L_∞ attacks (Kurakin, Goodfellow, and Bengio 2016b; Carlini and Wagner 2017b), EAD can attain similar attack success rate when breaking undefended and defensively distilled DNNs (Papernot et al. 2016b). More importantly, we find that L_1 attacks attain superior performance over L_2 and L_∞ attacks in transfer attacks and complement adversarial training. For the most difficult dataset (MNIST), EAD results in improved attack transferability from an undefended DNN to a defensively distilled DNN, achieving nearly 99% attack success rate. In addition, joint adversarial training with L_1 and L_2 -based examples can further enhance the resilience of DNNs to adversarial perturbations. These results suggest that EAD yields a distinct yet more effective set of adversarial examples. Moreover, evaluating attacks based on L_1 distortion provides novel insights on adversarial learning and security implications for DNNs, suggesting that L_1 may complement L_2 and L_∞ -based examples toward furthering a thorough adversarial learning framework.

Related Work

Here we summarize related works on attacking and defending DNNs against adversarial examples.

Attacks to DNNs

FGM and I-FGM: Let \mathbf{x}_0 and \mathbf{x} denote the original and adversarial examples, respectively, and let t denote the target class to attack. Fast gradient methods (FGM) use the gradient ∇J of the training loss J with respect to \mathbf{x}_0 for crafting adversarial examples (Goodfellow, Shlens, and Szegedy 2015). For L_∞ attacks, \mathbf{x} is crafted by

$$\mathbf{x} = \mathbf{x}_0 - \epsilon \cdot \text{sign}(\nabla J(\mathbf{x}_0, t)), \quad (1)$$

where ϵ specifies the L_∞ distortion between \mathbf{x} and \mathbf{x}_0 , and $\text{sign}(\nabla J)$ takes the sign of the gradient. For L_1 and L_2 at-

tacks, \mathbf{x} is crafted by

$$\mathbf{x} = \mathbf{x}_0 - \epsilon \frac{\nabla J(\mathbf{x}_0, t)}{\|\nabla J(\mathbf{x}_0, t)\|_q} \quad (2)$$

for $q = 1, 2$, where ϵ specifies the corresponding distortion. Iterative fast gradient methods (I-FGM) were proposed in (Kurakin, Goodfellow, and Bengio 2016b), which iteratively use FGM with a finer distortion, followed by an ϵ -ball clipping. Untargeted attacks using FGM and I-FGM can be implemented in a similar fashion.

C&W attack: Instead of leveraging the training loss, Carlini and Wagner designed an L_2 -regularized loss function based on the logit layer representation in DNNs for crafting adversarial examples (Carlini and Wagner 2017b). Its formulation turns out to be a special case of our EAD formulation, which will be discussed in the following section. The C&W attack is considered to be one of the strongest attacks to DNNs, as it can successfully break undefended and defensively distilled DNNs and can attain remarkable attack transferability.

JSMA: Papernot et al. proposed a Jacobian-based saliency map algorithm (JSMA) for characterizing the input-output relation of DNNs (Papernot et al. 2016a). It can be viewed as a greedy attack algorithm that iteratively modifies the most influential pixel for crafting adversarial examples.

DeepFool: DeepFool is an untargeted L_2 attack algorithm (Moosavi-Dezfooli, Fawzi, and Frossard 2016) based on the theory of projection to the closest separating hyperplane in classification. It is also used to craft a universal perturbation to mislead DNNs trained on natural images (Moosavi-Dezfooli et al. 2016).

Black-box attacks: Crafting adversarial examples in the black-box case is plausible if one allows querying of the target DNN. In (Papernot et al. 2017), JSMA is used to train a substitute model for transfer attacks. In (Chen et al. 2017), an effective black-box C&W attack is made possible using zeroth order optimization (ZOO). In the more stringent attack scenario where querying is prohibited, ensemble methods can be used for transfer attacks (Liu et al. 2016).

Defenses in DNNs

Defensive distillation: Defensive distillation (Papernot et al. 2016b) defends against adversarial perturbations by using the distillation technique in (Hinton, Vinyals, and Dean 2015) to retrain the network with class probabilities predicted by the original network. It also introduces the temperature parameter T in the softmax layer to enhance the robustness to adversarial perturbations.

Adversarial training: Adversarial training can be implemented in a few different ways. A standard approach is augmenting the original training dataset with the label-corrected adversarial examples to retrain the network. Modifying the training loss or the network architecture to increase the robustness of DNNs to adversarial examples has been proposed in (Zheng et al. 2016; Madry et al. 2017; Tramèr et al. 2017; Zantedeschi, Nicolae, and Rawat 2017).

Detection methods: Detection methods utilize statistical tests to differentiate adversarial from benign examples (Feinman et al. 2017; Grosse et al. 2017; Lu, Issaranoon, and

Forsyth 2017; Xu, Evans, and Qi 2017). However, 10 different detection methods were unable to detect the C&W attack (Carlini and Wagner 2017a).

EAD: Elastic-Net Attacks to DNNs

Preliminaries on Elastic-Net Regularization

Elastic-net regularization is a widely used technique in solving high-dimensional feature selection problems (Zou and Hastie 2005). It can be viewed as a regularizer that linearly combines L_1 and L_2 penalty functions. In general, elastic-net regularization is used in the following minimization problem:

$$\text{minimize}_{\mathbf{z} \in \mathcal{Z}} f(\mathbf{z}) + \lambda_1 \|\mathbf{z}\|_1 + \lambda_2 \|\mathbf{z}\|_2^2, \quad (3)$$

where \mathbf{z} is a vector of p optimization variables, \mathcal{Z} indicates the set of feasible solutions, $f(\mathbf{z})$ denotes a loss function, $\|\mathbf{z}\|_q$ denotes the L_q norm of \mathbf{z} , and $\lambda_1, \lambda_2 \geq 0$ are the L_1 and L_2 regularization parameters, respectively. The term $\lambda_1 \|\mathbf{z}\|_1 + \lambda_2 \|\mathbf{z}\|_2^2$ in (3) is called the elastic-net regularizer of \mathbf{z} . For standard regression problems, the loss function $f(\mathbf{z})$ is the mean squared error, the vector \mathbf{z} represents the weights (coefficients) on the features, and the set $\mathcal{Z} = \mathbb{R}^p$. In particular, the elastic-net regularization in (3) degenerates to the LASSO formulation when $\lambda_2 = 0$, and becomes the ridge regression formulation when $\lambda_1 = 0$. It is shown in (Zou and Hastie 2005) that elastic-net regularization is able to select a group of highly correlated features, which overcomes the shortcoming of high-dimensional feature selection when solely using the LASSO or ridge regression techniques.

EAD Formulation and Generalization

Inspired by the C&W attack (Carlini and Wagner 2017b), we adopt the same loss function f for crafting adversarial examples. Specifically, given an image \mathbf{x}_0 and its correct label denoted by t_0 , let \mathbf{x} denote the adversarial example of \mathbf{x}_0 with a target class $t \neq t_0$. The loss function $f(\mathbf{x})$ for targeted attacks is defined as

$$f(\mathbf{x}, t) = \max\{\max_{j \neq t} [\mathbf{Logit}(\mathbf{x})]_j - [\mathbf{Logit}(\mathbf{x})]_t, -\kappa\}, \quad (4)$$

where $\mathbf{Logit}(\mathbf{x}) = [[\mathbf{Logit}(\mathbf{x})]_1, \dots, [\mathbf{Logit}(\mathbf{x})]_K] \in \mathbb{R}^K$ is the logit layer (the layer prior to the softmax layer) representation of \mathbf{x} in the considered DNN, K is the number of classes for classification, and $\kappa \geq 0$ is a confidence parameter that guarantees a constant gap between $\max_{j \neq t} [\mathbf{Logit}(\mathbf{x})]_j$ and $[\mathbf{Logit}(\mathbf{x})]_t$.

It is worth noting that the term $[\mathbf{Logit}(\mathbf{x})]_t$ is proportional to the probability of predicting \mathbf{x} as label t , since by the softmax classification rule,

$$\text{Prob}(\text{Label}(\mathbf{x}) = t) = \frac{\exp([\mathbf{Logit}(\mathbf{x})]_t)}{\sum_{j=1}^K \exp([\mathbf{Logit}(\mathbf{x})]_j)}. \quad (5)$$

Consequently, the loss function in (4) aims to render the label t the most probable class for \mathbf{x} , and the parameter κ controls the separation between t and the next most likely prediction among all classes other than t . For untargeted attacks, the loss function in (4) can be modified as

$$f(\mathbf{x}) = \max\{[\mathbf{Logit}(\mathbf{x})]_{t_0} - \max_{j \neq t} [\mathbf{Logit}(\mathbf{x})]_j, -\kappa\}. \quad (6)$$

In this paper, we focus on targeted attacks since they are more challenging than untargeted attacks. Our EAD algorithm (Algorithm 1) can directly be applied to untargeted attacks by replacing $f(\mathbf{x}, t)$ in (4) with $f(\mathbf{x})$ in (6).

In addition to manipulating the prediction via the loss function in (4), introducing elastic-net regularization further encourages similarity to the original image when crafting adversarial examples. Our formulation of elastic-net attacks to DNNs (EAD) for crafting an adversarial example (\mathbf{x}, t) with respect to a labeled normal image (\mathbf{x}_0, t_0) is as follows:

$$\begin{aligned} &\text{minimize}_{\mathbf{x}} \quad c \cdot f(\mathbf{x}, t) + \beta \|\mathbf{x} - \mathbf{x}_0\|_1 + \|\mathbf{x} - \mathbf{x}_0\|_2^2 \\ &\text{subject to} \quad \mathbf{x} \in [0, 1]^p, \end{aligned} \quad (7)$$

where $f(\mathbf{x}, t)$ is as defined in (4), $c, \beta \geq 0$ are the regularization parameters of the loss function f and the L_1 penalty, respectively. The box constraint $\mathbf{x} \in [0, 1]^p$ restricts \mathbf{x} to a properly scaled image space, which can be easily satisfied by dividing each pixel value by the maximum attainable value (e.g., 255). Upon defining the perturbation of \mathbf{x} relative to \mathbf{x}_0 as $\delta = \mathbf{x} - \mathbf{x}_0$, the EAD formulation in (7) aims to find an adversarial example \mathbf{x} that will be classified as the target class t while minimizing the distortion in δ in terms of the elastic-net loss $\beta \|\delta\|_1 + \|\delta\|_2^2$, which is a linear combination of L_1 and L_2 distortion metrics between \mathbf{x} and \mathbf{x}_0 . Notably, the formulation of the C&W attack (Carlini and Wagner 2017b) becomes a special case of the EAD formulation in (7) when $\beta = 0$, which disregards the L_1 penalty on δ . However, the L_1 penalty is an intuitive regularizer for crafting adversarial examples, as $\|\delta\|_1 = \sum_{i=1}^p |\delta_i|$ represents the total variation of the perturbation, and is also a widely used surrogate function for promoting sparsity in the perturbation. As will be evident in the performance evaluation section, including the L_1 penalty for the perturbation indeed yields a distinct set of adversarial examples, and it leads to improved attack transferability and complements adversarial learning.

EAD Algorithm

When solving the EAD formulation in (7) without the L_1 penalty (i.e., $\beta = 0$), Carlini and Wagner used a change-of-variable (COV) approach via the tanh transformation on \mathbf{x} in order to remove the box constraint $\mathbf{x} \in [0, 1]^p$ (Carlini and Wagner 2017b). When $\beta > 0$, we find that the same COV approach is not effective in solving (7), since the corresponding adversarial examples are insensitive to the changes in β (see the performance evaluation section for details). Since the L_1 penalty is a non-differentiable yet smooth function, the failure of the COV approach in solving (7) can be explained by its inefficiency in subgradient-based optimization problems (Duchi and Singer 2009).

To efficiently solve the EAD formulation in (7) for crafting adversarial examples, we propose to use the iterative shrinkage-thresholding algorithm (ISTA) (Beck and Teboulle 2009). ISTA can be viewed as a regular first-order optimization algorithm with an additional shrinkage-thresholding step on each iteration. In particular, let $g(\mathbf{x}) = c \cdot f(\mathbf{x}) + \|\mathbf{x} - \mathbf{x}_0\|_2^2$ and let $\nabla g(\mathbf{x})$ be the numerical gradient of $g(\mathbf{x})$ computed by the DNN. At the $k + 1$ -th iteration, the

Algorithm 1 Elastic-Net Attacks to DNNs (EAD)

Input: original labeled image (\mathbf{x}_0, t_0) , target attack class t , attack transferability parameter κ , L_1 regularization parameter β , step size α_k , # of iterations I

Output: adversarial example \mathbf{x}

Initialization: $\mathbf{x}^{(0)} = \mathbf{y}^{(0)} = \mathbf{x}_0$

for $k = 0$ to $I - 1$ **do**

$$\mathbf{x}^{(k+1)} = S_\beta(\mathbf{y}^{(k)} - \alpha_k \nabla g(\mathbf{y}^{(k)}))$$

$$\mathbf{y}^{(k+1)} = \mathbf{x}^{(k+1)} + \frac{k}{k+3}(\mathbf{x}^{(k+1)} - \mathbf{x}^{(k)})$$

end for

Decision rule: determine \mathbf{x} from successful examples in $\{\mathbf{x}^{(k)}\}_{k=1}^I$ (EN rule or L_1 rule).

adversarial example $\mathbf{x}^{(k+1)}$ of \mathbf{x}_0 is computed by

$$\mathbf{x}^{(k+1)} = S_\beta(\mathbf{x}^{(k)} - \alpha_k \nabla g(\mathbf{x}^{(k)})), \quad (8)$$

where α_k denotes the step size at the $k + 1$ -th iteration, and $S_\beta : \mathbb{R}^p \mapsto \mathbb{R}^p$ is an element-wise projected shrinkage-thresholding function, which is defined as

$$[S_\beta(\mathbf{z})]_i = \begin{cases} \min\{\mathbf{z}_i - \beta, 1\}, & \text{if } \mathbf{z}_i - \mathbf{x}_{0i} > \beta; \\ \mathbf{x}_{0i}, & \text{if } |\mathbf{z}_i - \mathbf{x}_{0i}| \leq \beta; \\ \max\{\mathbf{z}_i + \beta, 0\}, & \text{if } \mathbf{z}_i - \mathbf{x}_{0i} < -\beta, \end{cases} \quad (9)$$

for any $i \in \{1, \dots, p\}$. If $|\mathbf{z}_i - \mathbf{x}_{0i}| > \beta$, it shrinks the element \mathbf{z}_i by β and projects the resulting element to the feasible box constraint between 0 and 1. On the other hand, if $|\mathbf{z}_i - \mathbf{x}_{0i}| \leq \beta$, it thresholds \mathbf{z}_i by setting $[S_\beta(\mathbf{z})]_i = \mathbf{x}_{0i}$. The proof of optimality of using (8) for solving the EAD formulation in (7) is given in the supplementary material. Notably, since $g(\mathbf{x})$ is the attack objective function of the C&W method (Carlini and Wagner 2017b), the ISTA operation in (8) can be viewed as a robust version of the C&W method that shrinks a pixel value of the adversarial example if the deviation to the original image is greater than β , and keeps a pixel value unchanged if the deviation is less than β .

Our EAD algorithm for crafting adversarial examples is summarized in Algorithm 1. For computational efficiency, a fast ISTA (FISTA) for EAD is implemented, which yields the optimal convergence rate for first-order optimization methods (Beck and Teboulle 2009). The slack vector $\mathbf{y}^{(k)}$ in Algorithm 1 incorporates the momentum in $\mathbf{x}^{(k)}$ for acceleration. In the experiments, we set the initial learning rate $\alpha_0 = 0.01$ with a square-root decay factor in k . During the EAD iterations, the iterate $\mathbf{x}^{(k)}$ is considered as a successful adversarial example of \mathbf{x}_0 if the model predicts its most likely class to be the target class t . The final adversarial example \mathbf{x} is selected from all successful examples based on distortion metrics. In this paper we consider two decision rules for selecting \mathbf{x} : the least elastic-net (EN) and L_1 distortions relative to \mathbf{x}_0 . The influence of β , κ and the decision rules on EAD will be investigated in the following section.

Performance Evaluation

In this section, we compare the proposed EAD with the state-of-the-art attacks to DNNs on three image classification datasets - MNIST, CIFAR10 and ImageNet. We would

like to show that (i) EAD can attain attack performance similar to the C&W attack in breaking undefended and defensively distilled DNNs, since the C&W attack is a special case of EAD when $\beta = 0$; (ii) Comparing to existing L_1 -based FGM and I-FGM methods, the adversarial examples using EAD can lead to significantly lower L_1 distortion and better attack success rate; (iii) The L_1 -based adversarial examples crafted by EAD can achieve improved attack transferability and complement adversarial training.

Comparative Methods

We compare EAD with the following targeted attacks, which are the most effective methods for crafting adversarial examples in different distortion metrics.

C&W attack: The state-of-the-art L_2 targeted attack proposed by Carlini and Wagner (Carlini and Wagner 2017b), which is a special case of EAD when $\beta = 0$.

FGM: The fast gradient method proposed in (Goodfellow, Shlens, and Szegedy 2015). The FGM attacks using different distortion metrics are denoted by FGM- L_1 , FGM- L_2 and FGM- L_∞ .

I-FGM: The iterative fast gradient method proposed in (Kurakin, Goodfellow, and Bengio 2016b). The I-FGM attacks using different distortion metrics are denoted by I-FGM- L_1 , I-FGM- L_2 and I-FGM- L_∞ .

Experiment Setup and Parameter Setting

Our experiment setup is based on Carlini and Wagner's framework¹. For both the EAD and C&W attacks, we use the default setting¹, which implements 9 binary search steps on the regularization parameter c (starting from 0.01) and runs $I = 1000$ iterations for each step with the initial learning rate $\alpha_0 = 0.01$. For finding successful adversarial examples, we use the reference optimizer¹ (ADAM) for the C&W attack and implement the projected FISTA (Algorithm 1) with the square-root decaying learning rate for EAD. Similar to the C&W attack, the final adversarial example of EAD is selected by the least distorted example among all the successful examples. The sensitivity analysis of the L_1 parameter β and the effect of the decision rule on EAD will be investigated in the forthcoming paragraph. Unless specified, we set the attack transferability parameter $\kappa = 0$ for both attacks.

We implemented FGM and I-FGM using the CleverHans package². The best distortion parameter ϵ is determined by a fine-grained grid search - for each image, the smallest ϵ in the grid leading to a successful attack is reported. For I-FGM, we perform 10 FGM iterations (the default value) with ϵ -ball clipping. The distortion parameter ϵ' in each FGM iteration is set to be $\epsilon/10$, which has been shown to be an effective attack setting in (Tramèr et al. 2017). The range of the grid and the resolution of these two methods are specified in Table 4 in the supplementary material.

The image classifiers for MNIST and CIFAR10 are trained based on the DNN models provided by Carlini and

¹https://github.com/carlini/nn_robust_attacks

²<https://github.com/tensorflow/cleverhans/blob/master/cleverhans/attacks.py>

Table 1: Comparison of the change-of-variable (COV) approach and EAD (Algorithm 1) for solving the elastic-net formulation in (7) on MNIST. ASR means attack success rate (%). Although these two methods attain similar attack success rates, COV is not effective in crafting L_1 -based adversarial examples. Increasing β leads to less L_1 -distorted adversarial examples for EAD, whereas the distortion of COV is insensitive to changes in β .

Optimization method	β	Best case				Average case				Worst case			
		ASR	L_1	L_2	L_∞	ASR	L_1	L_2	L_∞	ASR	L_1	L_2	L_∞
COV	0	100	13.93	1.377	0.379	100	22.46	1.972	0.514	99.9	32.3	2.639	0.663
	10^{-5}	100	13.92	1.377	0.379	100	22.66	1.98	0.508	99.5	32.33	2.64	0.663
	10^{-4}	100	13.91	1.377	0.379	100	23.11	2.013	0.517	100	32.32	2.639	0.664
	10^{-3}	100	13.8	1.377	0.381	100	22.42	1.977	0.512	99.9	32.2	2.639	0.664
	10^{-2}	100	12.98	1.38	0.389	100	22.27	2.026	0.53	99.5	31.41	2.643	0.673
EAD (EN rule)	0	100	14.04	1.369	0.376	100	22.63	1.953	0.512	99.8	31.43	2.51	0.644
	10^{-5}	100	13.66	1.369	0.378	100	22.6	1.98	0.515	99.9	30.79	2.507	0.648
	10^{-4}	100	12.79	1.372	0.388	100	20.98	1.951	0.521	100	29.21	2.514	0.667
	10^{-3}	100	9.808	1.427	0.452	100	17.4	2.001	0.594	100	25.52	2.582	0.748
	10^{-2}	100	7.271	1.718	0.674	100	13.56	2.395	0.852	100	20.77	3.021	0.976

Wagner¹. The image classifier for ImageNet is the Inception-v3 model (Szegedy et al. 2016). For MNIST and CIFAR10, 1000 correctly classified images are randomly selected from the test sets to attack an incorrect class label. For ImageNet, 100 correctly classified images and 9 incorrect classes are randomly selected to attack. All experiments are conducted on a machine with an Intel E5-2690 v3 CPU, 40 GB RAM and a single NVIDIA K80 GPU. Our EAD code is publicly available for download³.

Evaluation Metrics

Following the attack evaluation criterion in (Carlini and Wagner 2017b), we report the attack success rate and distortion of the adversarial examples from each method. The attack success rate (ASR) is defined as the percentage of adversarial examples that are classified as the target class (which is different from the original class). The average L_1 , L_2 and L_∞ distortion metrics of successful adversarial examples are also reported. In particular, the ASR and distortion of the following attack settings are considered:

Best case: The least difficult attack among targeted attacks to all incorrect class labels in terms of distortion.

Average case: The targeted attack to a randomly selected incorrect class label.

Worst case: The most difficult attack among targeted attacks to all incorrect class labels in terms of distortion.

Sensitivity Analysis and Decision Rule for EAD

We verify the necessity of using Algorithm 1 for solving the elastic-net regularized attack formulation in (7) by comparing it to a naive change-of-variable (COV) approach. In (Carlini and Wagner 2017b), Carlini and Wagner remove the box constraint $\mathbf{x} \in [0, 1]^p$ by replacing \mathbf{x} with $\frac{\mathbf{1} + \tanh \mathbf{w}}{2}$, where $\mathbf{w} \in \mathbb{R}^p$ and $\mathbf{1} \in \mathbb{R}^p$ is a vector of ones. The default ADAM optimizer (Kingma and Ba 2014) is then used to solve \mathbf{w} and obtain \mathbf{x} . We apply this COV approach to (7) and compare with EAD on MNIST with different orders

of the L_1 regularization parameter β in Table 1. Although COV and EAD attain similar attack success rates, it is observed that COV is not effective in crafting L_1 -based adversarial examples. Increasing β leads to less L_1 -distorted adversarial examples for EAD, whereas the distortion (L_1 , L_2 and L_∞) of COV is insensitive to changes in β . Similar insensitivity of COV on β is observed when one uses other optimizers such as AdaGrad, RMSProp or built-in SGD in TensorFlow. We also note that the COV approach prohibits the use of ISTA due to the subsequent \tanh term in the L_1 penalty. The insensitivity of COV suggests that it is inadequate for elastic-net optimization, which can be explained by its inefficiency in subgradient-based optimization problems (Duchi and Singer 2009). For EAD, we also find an interesting trade-off between L_1 and the other two distortion metrics - adversarial examples with smaller L_1 distortion tend to have larger L_2 and L_∞ distortions. This trade-off can be explained by the fact that increasing β further encourages sparsity in the perturbation, and hence results in increased L_2 and L_∞ distortion. Similar results are observed on CIFAR10 (see supplementary material).

In Table 1, during the attack optimization process the final adversarial example is selected based on the elastic-net loss of all successful adversarial examples in $\{\mathbf{x}^{(k)}\}_{k=1}^I$, which we call the *elastic-net (EN) decision rule*. Alternatively, we can select the final adversarial example with the least L_1 distortion, which we call the *L_1 decision rule*. Figure 2 compares the ASR and average-case distortion of these two decision rules with different β on MNIST. Both decision rules yield 100% ASR for a wide range of β values. For the same β , the L_1 rule gives adversarial examples with less L_1 distortion than those given by the EN rule at the price of larger L_2 and L_∞ distortions. Similar trends are observed on CIFAR10 (see supplementary material). The complete results of these two rules on MNIST and CIFAR10 are given in the supplementary material. In the following experiments, we will report the results of EAD with these two decision rules and set $\beta = 10^{-3}$, since on MNIST and CIFAR10 this β

³<https://github.com/ysharma1126/EAD-Attack>

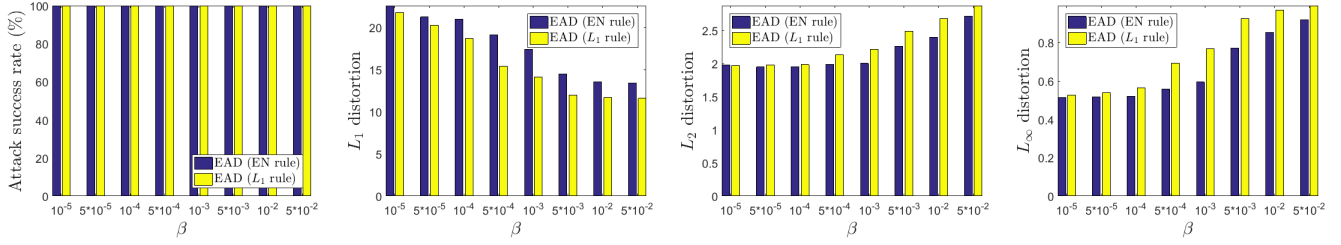


Figure 2: Comparison of EN and L_1 decision rules in EAD on MNIST with varying L_1 regularization parameter β (average case). Comparing to the EN rule, for the same β the L_1 rule attains less L_1 distortion but may incur more L_2 and L_∞ distortions.

Table 2: Comparison of different attacks on MNIST, CIFAR10 and ImageNet (average case). ASR means attack success rate (%). The distortion metrics are averaged over successful examples. EAD, the C&W attack, and I-FGM- L_∞ attain the least L_1 , L_2 , and L_∞ distorted adversarial examples, respectively. The complete attack results are given in the supplementary material.

Attack method	MNIST				CIFAR10				ImageNet			
	ASR	L_1	L_2	L_∞	ASR	L_1	L_2	L_∞	ASR	L_1	L_2	L_∞
C&W (L_2)	100	22.46	1.972	0.514	100	13.62	0.392	0.044	100	232.2	0.705	0.03
FGM- L_1	39	53.5	4.186	0.782	48.8	51.97	1.48	0.152	1	61	0.187	0.007
FGM- L_2	34.6	39.15	3.284	0.747	42.8	39.5	1.157	0.136	1	2338	6.823	0.25
FGM- L_∞	42.5	127.2	6.09	0.296	52.3	127.81	2.373	0.047	3	3655	7.102	0.014
I-FGM- L_1	100	32.94	2.606	0.591	100	17.53	0.502	0.055	77	526.4	1.609	0.054
I-FGM- L_2	100	30.32	2.41	0.561	100	17.12	0.489	0.054	100	774.1	2.358	0.086
I-FGM- L_∞	100	71.39	3.472	0.227	100	33.3	0.68	0.018	100	864.2	2.079	0.01
EAD (EN rule)	100	17.4	2.001	0.594	100	8.18	0.502	0.097	100	69.47	1.563	0.238
EAD (L_1 rule)	100	14.11	2.211	0.768	100	6.066	0.613	0.17	100	40.9	1.598	0.293

value significantly reduces the L_1 distortion while having comparable L_2 and L_∞ distortions to the case of $\beta = 0$ (i.e., without L_1 regularization).

Attack Success Rate and Distortion on MNIST, CIFAR10 and ImageNet

We compare EAD with the comparative methods in terms of attack success rate and different distortion metrics on attacking the considered DNNs trained on MNIST, CIFAR10 and ImageNet. Table 2 summarizes their average-case performance. It is observed that FGM methods fail to yield successful adversarial examples (i.e., low ASR), and the corresponding distortion metrics are significantly larger than other methods. On the other hand, the C&W attack, I-FGM and EAD all lead to 100% attack success rate. Furthermore, EAD, the C&W method, and I-FGM- L_∞ attain the least L_1 , L_2 , and L_∞ distorted adversarial examples, respectively. We note that EAD significantly outperforms the existing L_1 -based method (I-FGM- L_1). Compared to I-FGM- L_1 , EAD with the EN decision rule reduces the L_1 distortion by roughly 47% on MNIST, 53% on CIFAR10 and 87% on ImageNet. We also observe that EAD with the L_1 decision rule can further reduce the L_1 distortion but at the price of noticeable increase in the L_2 and L_∞ distortion metrics.

Notably, despite having large L_2 and L_∞ distortion metrics, the adversarial examples crafted by EAD with the L_1 rule can still attain 100% ASRs in all datasets, which implies the L_2 and L_∞ distortion metrics are insufficient for evaluating the robustness of neural networks. Moreover, the

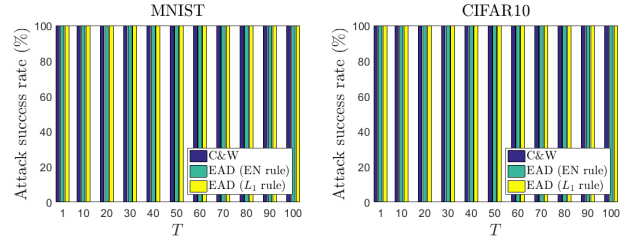


Figure 3: Attack success rate (average case) of the C&W method and EAD on MNIST and CIFAR10 with respect to varying temperature parameter T for defensive distillation. Both methods can successfully break defensive distillation.

attack results in Table 2 suggest that EAD can yield a set of distinct adversarial examples that are fundamentally different from L_2 or L_∞ based examples. Similar to the C&W method and I-FGM, the adversarial examples from EAD are also visually indistinguishable (see supplementary material).

Breaking Defensive Distillation

In addition to breaking undefended DNNs via adversarial examples, here we show that EAD can also break defensively distilled DNNs. Defensive distillation (Papernot et al. 2016b) is a standard defense technique that retrain the network with class label probabilities predicted by the original network, soft labels, and introduces the temperature parameter T in the softmax layer to enhance its robustness to adver-

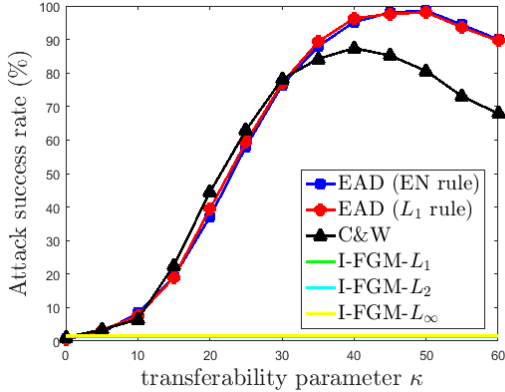


Figure 4: Attack transferability (average case) from the undefended network to the defensively distilled network on MNIST by varying κ . EAD can attain nearly 99% attack success rate (ASR) when $\kappa = 50$, whereas the top ASR of the C&W attack is nearly 88% when $\kappa = 40$.

serial perturbations. Similar to the state-of-the-art attack (the C&W method), Figure 3 shows that EAD can attain 100% attack success rate for different values of T on MNIST and CIFAR10. Moreover, since the C&W attack formulation is a special case of the EAD formulation in (7) when $\beta = 0$, successfully breaking defensive distillation using EAD suggests new ways of crafting effective adversarial examples by varying the L_1 regularization parameter β . The complete attack results are given in the supplementary material.

Improved Attack Transferability

It has been shown in (Carlini and Wagner 2017b) that the C&W attack can be made highly transferable from an undefended network to a defensively distilled network by tuning the confidence parameter κ in (4). Following (Carlini and Wagner 2017b), we adopt the same experiment setting for attack transferability on MNIST, as MNIST is the most difficult dataset to attack in terms of the average distortion per image pixel from Table 2.

Fixing κ , adversarial examples generated from the original (undefended) network are used to attack the defensively distilled network with the temperature parameter $T = 100$ (Papernot et al. 2016b). The attack success rate (ASR) of EAD, the C&W method and I-FGM are shown in Figure 4. When $\kappa = 0$, all methods attain low ASR and hence do not produce transferable adversarial examples. The ASR of EAD and the C&W method improves when we set $\kappa > 0$, whereas I-FGM’s ASR remains low (less than 2%) since the attack does not have such a parameter for transferability.

Notably, EAD can attain nearly 99% ASR when $\kappa = 50$, whereas the top ASR of the C&W method is nearly 88% when $\kappa = 40$. This implies improved attack transferability when using the adversarial examples crafted by EAD, which can be explained by the fact that the ISTA operation in (8) is a robust version of the C&W attack via shrinking and thresholding. We also find that setting κ too large may mitigate the ASR of transfer attacks for both EAD and the

Table 3: Adversarial training using the C&W attack and EAD (L_1 rule) on MNIST. ASR means attack success rate. Incorporating L_1 examples complements adversarial training and enhances attack difficulty in terms of distortion. The complete results are given in the supplementary material.

Attack method	Adversarial training	Average case			
		ASR	L_1	L_2	L_∞
C&W (L_2)	None	100	22.46	1.972	0.514
	EAD	100	26.11	2.468	0.643
	C&W	100	24.97	2.47	0.684
	EAD + C&W	100	27.32	2.513	0.653
EAD (L_1 rule)	None	100	14.11	2.211	0.768
	EAD	100	17.04	2.653	0.86
	C&W	100	15.49	2.628	0.892
	EAD + C&W	100	16.83	2.66	0.87

C&W method, as the optimizer may fail to find an adversarial example that minimizes the loss function f in (4) for large κ . The complete attack transferability results are given in the supplementary material.

Complementing Adversarial Training

To further validate the difference between L_1 -based and L_2 -based adversarial examples, we test their performance in adversarial training on MNIST. We randomly select 1000 images from the training set and use the C&W attack and EAD (L_1 rule) to generate adversarial examples for all incorrect labels, leading to 9000 adversarial examples in total for each method. We then separately augment the original training set with these examples to retrain the network and test its robustness on the testing set, as summarized in Table 3. For adversarial training with any single method, although both attacks still attain a 100% success rate in the average case, the network is more tolerable to adversarial perturbations, as all distortion metrics increase significantly when compared to the null case. We also observe that joint adversarial training with EAD and the C&W method can further increase the L_1 and L_2 distortions against the C&W attack and the L_2 distortion against EAD, suggesting that the L_1 -based examples crafted by EAD can complement adversarial training.

Conclusion

We proposed an elastic-net regularized attack framework for crafting adversarial examples to attack deep neural networks. Experimental results on MNIST, CIFAR10 and ImageNet show that the L_1 -based adversarial examples crafted by EAD can be as successful as the state-of-the-art L_2 and L_∞ attacks in breaking undefended and defensively distilled networks. Furthermore, EAD can improve attack transferability and complement adversarial training. Our findings shed new light on the use of L_1 -based adversarial examples toward adversarial learning and security implications in deep neural networks.

References

- Beck, A., and Teboulle, M. 2009. A fast iterative shrinkage-thresholding algorithm for linear inverse problems. *SIAM journal on imaging sciences* 2(1):183–202.
- Candès, E. J., and Wakin, M. B. 2008. An introduction to compressive sampling. *IEEE signal processing magazine* 25(2):21–30.
- Carlini, N., and Wagner, D. 2017a. Adversarial examples are not easily detected: Bypassing ten detection methods. *arXiv preprint arXiv:1705.07263*.
- Carlini, N., and Wagner, D. 2017b. Towards evaluating the robustness of neural networks. In *IEEE Symposium on Security and Privacy (SP)*, 39–57.
- Chen, P.-Y.; Zhang, H.; Sharma, Y.; Yi, J.; and Hsieh, C.-J. 2017. Zoo: Zeroth order optimization based black-box attacks to deep neural networks without training substitute models. *arXiv preprint arXiv:1708.03999*.
- Dong, Y.; Su, H.; Zhu, J.; and Bao, F. 2017. Towards interpretable deep neural networks by leveraging adversarial examples. *arXiv preprint arXiv:1708.05493*.
- Duchi, J., and Singer, Y. 2009. Efficient online and batch learning using forward backward splitting. *Journal of Machine Learning Research* 10(Dec):2899–2934.
- Evtimov, I.; Eykholt, K.; Fernandes, E.; Kohno, T.; Li, B.; Prakash, A.; Rahmati, A.; and Song, D. 2017. Robust physical-world attacks on machine learning models. *arXiv preprint arXiv:1707.08945*.
- Feinman, R.; Curtin, R. R.; Shintre, S.; and Gardner, A. B. 2017. Detecting adversarial samples from artifacts. *arXiv preprint arXiv:1703.00410*.
- Fu, H.; Ng, M. K.; Nikolova, M.; and Barlow, J. L. 2006. Efficient minimization methods of mixed l2-l1 and l1-l1 norms for image restoration. *SIAM Journal on scientific computing* 27(6):1881–1902.
- Goodfellow, I. J.; Shlens, J.; and Szegedy, C. 2015. Explaining and harnessing adversarial examples. *ICLR’15; arXiv preprint arXiv:1412.6572*.
- Grosse, K.; Manoharan, P.; Papernot, N.; Backes, M.; and McDaniel, P. 2017. On the (statistical) detection of adversarial examples. *arXiv preprint arXiv:1702.06280*.
- Hinton, G.; Vinyals, O.; and Dean, J. 2015. Distilling the knowledge in a neural network. *arXiv preprint arXiv:1503.02531*.
- Kingma, D., and Ba, J. 2014. Adam: A method for stochastic optimization. *arXiv preprint arXiv:1412.6980*.
- Koh, P. W., and Liang, P. 2017. Understanding black-box predictions via influence functions. *ICML; arXiv preprint arXiv:1703.04730*.
- Kurakin, A.; Goodfellow, I.; and Bengio, S. 2016a. Adversarial examples in the physical world. *arXiv preprint arXiv:1607.02533*.
- Kurakin, A.; Goodfellow, I.; and Bengio, S. 2016b. Adversarial machine learning at scale. *ICLR’17; arXiv preprint arXiv:1611.01236*.
- Liu, Y.; Chen, X.; Liu, C.; and Song, D. 2016. Delving into transferable adversarial examples and black-box attacks. *arXiv preprint arXiv:1611.02770*.
- Lu, J.; Issararanon, T.; and Forsyth, D. 2017. Safetynet: Detecting and rejecting adversarial examples robustly. *arXiv preprint arXiv:1704.00103*.
- Madry, A.; Makelov, A.; Schmidt, L.; Tsipras, D.; and Vladu, A. 2017. Towards deep learning models resistant to adversarial attacks. *arXiv preprint arXiv:1706.06083*.
- Moosavi-Dezfooli, S.-M.; Fawzi, A.; Fawzi, O.; and Frossard, P. 2016. Universal adversarial perturbations. *arXiv preprint arXiv:1610.08401*.
- Moosavi-Dezfooli, S.-M.; Fawzi, A.; and Frossard, P. 2016. Deepfool: a simple and accurate method to fool deep neural networks. In *Proceedings of the IEEE Conference on Computer Vision and Pattern Recognition*, 2574–2582.
- Papernot, N.; McDaniel, P.; Jha, S.; Fredrikson, M.; Celik, Z. B.; and Swami, A. 2016a. The limitations of deep learning in adversarial settings. In *IEEE European Symposium on Security and Privacy (EuroS&P)*, 372–387.
- Papernot, N.; McDaniel, P.; Wu, X.; Jha, S.; and Swami, A. 2016b. Distillation as a defense to adversarial perturbations against deep neural networks. In *IEEE Symposium on Security and Privacy (SP)*, 582–597.
- Papernot, N.; McDaniel, P.; Goodfellow, I.; Jha, S.; Celik, Z. B.; and Swami, A. 2017. Practical black-box attacks against machine learning. In *ACM Asia Conference on Computer and Communications Security*, 506–519.
- Parikh, N.; Boyd, S.; et al. 2014. Proximal algorithms. *Foundations and Trends® in Optimization* 1(3):127–239.
- Szegedy, C.; Zaremba, W.; Sutskever, I.; Bruna, J.; Erhan, D.; Goodfellow, I.; and Fergus, R. 2013. Intriguing properties of neural networks. *arXiv preprint arXiv:1312.6199*.
- Szegedy, C.; Vanhoucke, V.; Ioffe, S.; Shlens, J.; and Wojna, Z. 2016. Rethinking the inception architecture for computer vision. In *Proceedings of the IEEE Conference on Computer Vision and Pattern Recognition*, 2818–2826.
- Tramèr, F.; Kurakin, A.; Papernot, N.; Boneh, D.; and McDaniel, P. 2017. Ensemble adversarial training: Attacks and defenses. *arXiv preprint arXiv:1705.07204*.
- Xu, W.; Evans, D.; and Qi, Y. 2017. Feature squeezing: Detecting adversarial examples in deep neural networks. *arXiv preprint arXiv:1704.01155*.
- Zantedeschi, V.; Nicolae, M.-I.; and Rawat, A. 2017. Efficient defenses against adversarial attacks. *arXiv preprint arXiv:1707.06728*.
- Zheng, S.; Song, Y.; Leung, T.; and Goodfellow, I. 2016. Improving the robustness of deep neural networks via stability training. In *Proceedings of the IEEE Conference on Computer Vision and Pattern Recognition*, 4480–4488.
- Zou, H., and Hastie, T. 2005. Regularization and variable selection via the elastic net. *Journal of the Royal Statistical Society: Series B (Statistical Methodology)* 67(2):301–320.

Supplementary Material

Proof of Optimality of (8) for Solving EAD in (3)

Since the L_1 penalty $\beta\|\mathbf{x} - \mathbf{x}_0\|_1$ in (3) is a non-differentiable yet smooth function, we use the proximal gradient method (Parikh, Boyd, and others 2014) for solving the EAD formulation in (3). Define $\Phi_{\mathcal{Z}}(\mathbf{z})$ to be the indicator function of an interval \mathcal{Z} such that $\Phi_{\mathcal{Z}}(\mathbf{z}) = 0$ if $\mathbf{z} \in \mathcal{Z}$ and $\Phi_{\mathcal{Z}}(\mathbf{z}) = \infty$ if $\mathbf{z} \notin \mathcal{Z}$. Using $\Phi_{\mathcal{Z}}(\mathbf{z})$, the EAD formulation in (3) can be rewritten as

$$\text{minimize}_{\mathbf{x} \in \mathbb{R}^p} g(\mathbf{x}) + \beta\|\mathbf{x} - \mathbf{x}_0\|_1 + \Phi_{[0,1]^p}(\mathbf{x}), \quad (10)$$

where $g(\mathbf{x}) = c \cdot f(\mathbf{x}, t) + \|\mathbf{x} - \mathbf{x}_0\|_2^2$. The proximal operator $\text{Prox}(\mathbf{x})$ of $\beta\|\mathbf{x} - \mathbf{x}_0\|_1$ constrained to $\mathbf{x} \in [0, 1]^p$ is

$$\begin{aligned} \text{Prox}(\mathbf{x}) &= \arg \min_{\mathbf{z} \in \mathbb{R}^p} \frac{1}{2}\|\mathbf{z} - \mathbf{x}\|_2^2 + \beta\|\mathbf{z} - \mathbf{x}_0\|_1 + \Phi_{[0,1]^p}(\mathbf{z}) \\ &= \arg \min_{\mathbf{z} \in [0,1]^p} \frac{1}{2}\|\mathbf{z} - \mathbf{x}\|_2^2 + \beta\|\mathbf{z} - \mathbf{x}_0\|_1 \\ &= S_{\beta}(\mathbf{x}), \end{aligned} \quad (11)$$

where the mapping function S_{β} is defined in (9). Consequently, using (11), the proximal gradient algorithm for solving (7) is iterated by

$$\mathbf{x}^{(k+1)} = \text{Prox}(\mathbf{x}^{(k)} - \alpha_k \nabla g(\mathbf{x}^{(k)})) \quad (12)$$

$$= S_{\beta}(\mathbf{x}^{(k)} - \alpha_k \nabla g(\mathbf{x}^{(k)})), \quad (13)$$

which completes the proof.

Grid Search for FGM and I-FGM (Table 4)

To determine the optimal distortion parameter ϵ for FGM and I-FGM methods, we adopt a fine grid search on ϵ . For each image, the best parameter is the smallest ϵ in the grid leading to a successful targeted attack. If the grid search fails to find a successful adversarial example, the attack is considered in vain. The selected range for grid search covers the reported distortion statistics of EAD and the C&W attack. The resolution of the grid search for FGM is selected such that it will generate 1000 candidates of adversarial examples during the grid search per input image. The resolution of the grid search for I-FGM is selected such that it will compute gradients for 10000 times in total (i.e., 1000 FGM operations \times 10 iterations) during the grid search per input image, which is more than the total number of gradients (9000) computed by EAD and the C&W attack.

Table 4: Range and resolution of grid search for finding the optimal distortion parameter ϵ for FGM and I-FGM.

Method	Grid search	
	Range	Resolution
FGM- L_{∞}	$[10^{-3}, 1]$	10^{-3}
FGM- L_1	$[1, 10^3]$	1
FGM- L_2	$[10^{-2}, 10]$	10^{-2}
I-FGM- L_{∞}	$[10^{-3}, 1]$	10^{-3}
I-FGM- L_1	$[1, 10^3]$	1
I-FGM- L_2	$[10^{-2}, 10]$	10^{-2}

Comparison of COV and EAD on CIFAR10 (Table 5)

Table 5 compares the attack performance of using EAD (Algorithm 1) and the change-of-variable (COV) approach for solving the elastic-net formulation in (7) on CIFAR10. Similar to the MNIST results in Table 1, although COV and EAD attain similar attack success rates, we find that COV is not effective in crafting L_1 -based adversarial examples. Increasing β leads to less L_1 -distorted adversarial examples for EAD, whereas the distortion (L_1 , L_2 and L_{∞}) of COV is insensitive to changes in β . The insensitivity of COV suggests that it is inadequate for elastic-net optimization, which can be explained by its inefficiency in subgradient-based optimization problems (Duchi and Singer 2009).

Comparison of EN and L_1 decision rules in EAD on MNIST and CIFAR10 (Tables 6 and 7)

Figure 5 compares the average-case distortion of these two decision rules with different values of β on CIFAR10. For the same β , the L_1 rule gives less L_1 distorted adversarial examples than those given by the EN rule at the price of larger L_2 and L_{∞} distortions. We also observe that the L_1 distortion does not decrease monotonically with β . In particular, large β values (e.g., $\beta = 5 \cdot 10^{-2}$) may lead to increased L_1 distortion due to excessive shrinking and thresholding. Table 6 and Table 7 displays the complete attack results of these two decision rules on MNIST and CIFAR10, respectively.

Complete Attack Results and Visual Illustration on MNIST, CIFAR10 and ImageNet (Tables 8, 9 and 10 and Figures 6, 7 and 8)

Tables 8, 9 and 10 summarize the complete attack results of all the considered attack methods on MNIST, CIFAR10 and ImageNet, respectively. EAD, the C&W attack and I-FGM all lead to 100% attack success rate in the average case. Among the three image classification datasets, ImageNet is the easiest one to attack due to low distortion per image pixel, and MNIST is the most difficult one to attack. For the purpose of visual illustration, the adversarial examples of selected benign images from the test sets are displayed in Figures 6, 7 and 8. On CIFAR10 and ImageNet, the adversarial examples are visually indistinguishable. On MNIST, the I-FGM examples are blurrier than EAD and the C&W attack.

Complete Results on Attacking Defensive Distillation on MNIST and CIFAR10 (Tables 11 and 12)

Tables 11 and 12 display the complete attack results of EAD and the C&W method on breaking defensive distillation with different temperature parameter T on MNIST and CIFAR10. Although defensive distillation is a standard defense technique for DNNs, EAD and the C&W attack can successfully break defensive distillation with a wide range of temperature parameters.

Table 5: Comparison of the change-of-variable (COV) approach and EAD (Algorithm 1) for solving the elastic-net formulation in (7) on CIFAR10. ASR means attack success rate (%). Similar to the results on MNIST in Table 1, increasing β leads to less L_1 -distorted adversarial examples for EAD, whereas the distortion of COV is insensitive to changes in β .

Optimization method	β	Best case				Average case				Worst case			
		ASR	L_1	L_2	L_∞	ASR	L_1	L_∞	L_∞	ASR	L_1	L_2	L_∞
COV	0	100	7.167	0.209	0.022	100	13.62	0.392	0.044	99.9	19.17	0.546	0.064
	10^{-5}	100	7.165	0.209	0.022	100	13.43	0.386	0.044	100	19.16	0.546	0.065
	10^{-4}	100	7.148	0.209	0.022	99.9	13.64	0.394	0.044	99.9	19.14	0.547	0.064
	10^{-3}	100	6.961	0.211	0.023	100	13.35	0.396	0.045	100	18.7	0.547	0.066
	10^{-2}	100	5.963	0.222	0.029	100	11.51	0.408	0.055	100	16.31	0.556	0.077
EAD (EN rule)	0	100	6.643	0.201	0.023	99.9	13.39	0.392	0.045	99.9	18.72	0.541	0.064
	10^{-5}	100	5.967	0.201	0.025	100	12.24	0.391	0.047	99.7	17.24	0.541	0.068
	10^{-4}	100	4.638	0.215	0.032	99.9	10.4	0.414	0.058	99.9	14.86	0.56	0.081
	10^{-3}	100	4.014	0.261	0.047	100	8.18	0.502	0.097	100	12.11	0.69	0.147
	10^{-2}	100	3.688	0.357	0.085	100	8.106	0.741	0.209	100	12.59	1.053	0.351

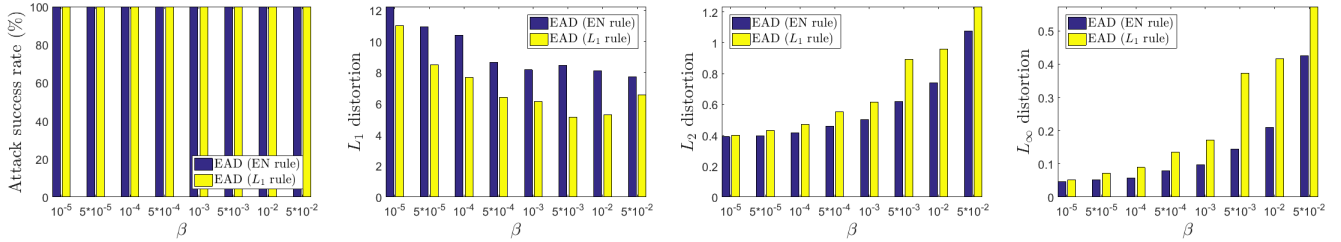


Figure 5: Comparison of EN and L_1 decision rules in EAD on CIFAR10 with varying L_1 regularization parameter β (average case). Comparing to the EN rule, for the same β the L_1 rule attains less L_1 distortion but may incur more L_2 and L_∞ distortions.

Complete Attack Transferability Results on MNIST (Table 13)

Table 13 summarizes the transfer attack results from an undefended DNN to a defensively distilled DNN on MNIST using EAD, the C&W attack and I-FGM. I-FGM methods have poor performance in attack transferability. The average attack success rate (ASR) of I-FGM is below 2%. On the other hand, adjusting the transferability parameter κ in EAD and the C&W attack can significantly improve ASR. Tested on a wide range of κ values, the top average-case ASR for EAD is 98.6% using the EN rule and 98.1% using the L_1 rule. The top average-case ASR for the C&W attack is 87.4%. This improvement is significantly due to the improvement in the worst case, where the top worst-case ASR for EAD is 87% using the EN rule and 85.8% using the L_1 rule, while the top worst-case ASR for the C&W attack is 30.5%. The results suggest that L_1 -based adversarial examples have better attack transferability.

Complete Results on Adversarial Training with L_1 and L_2 examples (Table 14)

Table 14 displays the complete results of adversarial training on MNIST using the L_2 -based adversarial examples crafted by the C&W attack and the L_1 -based adversarial examples crafted by EAD with the EN or the L_1 decision rule. It can be observed that adversarial training with any single method

can render the DNN more difficult to attack in terms of increased distortion metrics when compared with the null case. Notably, in the average case, joint adversarial training using L_1 and L_2 examples lead to increased L_1 and L_2 distortion against the C&W attack and EAD (EN), and increased L_2 distortion against EAD (L_1). The results suggest that EAD can complement adversarial training toward resilient DNNs. We would like to point out that in our experiments, adversarial training maintains comparable test accuracy. All the adversarially trained DNNs in Table 14 can still attain at least 99% test accuracy on MNIST.

Table 6: Comparison of the elastic net (EN) and L_1 decision rules in EAD for selecting adversarial examples on MNIST. ASR means attack success rate (%).

		Best case				Average case				Worst case			
Decision rule	β	ASR	L_1	L_2	L_∞	ASR	L_1	L_2	L_∞	ASR	L_1	L_2	L_∞
EAD (EN rule)	10^{-5}	100	13.66	1.369	0.378	100	22.6	1.98	0.515	99.9	30.79	2.507	0.648
	$5 \cdot 10^{-5}$	100	13.19	1.37	0.383	100	21.25	1.947	0.518	100	29.82	2.512	0.659
	10^{-4}	100	12.79	1.372	0.388	100	20.98	1.951	0.521	100	29.21	2.514	0.667
	$5 \cdot 10^{-4}$	100	10.95	1.395	0.42	100	19.11	1.986	0.558	100	27.04	2.544	0.706
	10^{-3}	100	9.808	1.427	0.452	100	17.4	2.001	0.594	100	25.52	2.582	0.748
	$5 \cdot 10^{-3}$	100	7.912	1.6	0.591	100	14.49	2.261	0.772	100	21.64	2.835	0.921
	10^{-2}	100	7.271	1.718	0.674	100	13.56	2.395	0.852	100	20.77	3.021	0.976
	$5 \cdot 10^{-2}$	100	7.088	1.872	0.736	100	13.38	2.712	0.919	100	20.19	3.471	0.998
EAD (L_1 rule)	10^{-5}	100	13.26	1.376	0.386	100	21.75	1.965	0.525	100	30.48	2.521	0.666
	$5 \cdot 10^{-4}$	100	11.81	1.385	0.404	100	20.28	1.98	0.54	100	28.8	2.527	0.686
	10^{-4}	100	10.75	1.403	0.424	100	18.69	1.983	0.565	100	27.49	2.539	0.71
	$5 \cdot 10^{-4}$	100	8.025	1.534	0.527	100	15.42	2.133	0.694	100	23.62	2.646	0.857
	10^{-3}	100	7.153	1.639	0.593	100	14.11	2.211	0.768	100	22.05	2.747	0.934
	$5 \cdot 10^{-3}$	100	6.347	1.844	0.772	100	11.99	2.491	0.927	100	18.01	3.218	0.997
	10^{-2}	100	6.193	1.906	0.861	100	11.69	2.68	0.97	100	17.29	3.381	1
	$5 \cdot 10^{-2}$	100	5.918	2.101	0.956	100	11.59	2.873	0.993	100	18.67	3.603	1

Table 7: Comparison of the elastic net (EN) and L_1 decision rules in EAD for selecting adversarial examples on CIFAR10. ASR means attack success rate (%).

		Best case				Average case				Worst case			
Decision rule	β	ASR	L_1	L_2	L_∞	ASR	L_1	L_2	L_∞	ASR	L_1	L_2	L_∞
EAD (EN rule)	10^{-5}	100	5.967	0.201	0.025	100	12.24	0.391	0.047	99.7	17.24	0.541	0.068
	$5 \cdot 10^{-5}$	100	5.09	0.207	0.028	99.9	10.94	0.396	0.052	99.9	15.87	0.549	0.075
	10^{-4}	100	4.638	0.215	0.032	99.9	10.4	0.414	0.058	99.9	14.86	0.56	0.081
	$5 \cdot 10^{-4}$	100	4.35	0.241	0.039	100	8.671	0.459	0.079	100	12.39	0.63	0.117
	10^{-3}	100	4.014	0.261	0.047	100	8.18	0.502	0.097	100	12.11	0.69	0.147
	$5 \cdot 10^{-3}$	100	3.83	0.319	0.067	100	8.462	0.619	0.145	100	13.03	0.904	0.255
	10^{-2}	100	3.688	0.357	0.085	100	8.106	0.741	0.209	100	12.59	1.053	0.351
	$5 \cdot 10^{-2}$	100	2.855	0.52	0.201	100	7.735	1.075	0.426	100	14.66	1.657	0.661
EAD (L_1 rule)	10^{-5}	100	5.002	0.209	0.029	100	11.03	0.4	0.052	99.8	16.03	0.548	0.074
	$5 \cdot 10^{-5}$	100	3.884	0.231	0.04	100	8.516	0.431	0.071	100	12.91	0.585	0.099
	10^{-4}	100	3.361	0.255	0.05	100	7.7	0.472	0.089	100	11.7	0.619	0.121
	$5 \cdot 10^{-4}$	100	2.689	0.339	0.091	100	6.414	0.552	0.135	100	10.11	0.732	0.192
	10^{-3}	100	2.6	0.358	0.103	100	6.127	0.617	0.171	100	8.99	0.874	0.272
	$5 \cdot 10^{-3}$	100	2.216	0.521	0.22	100	5.15	0.894	0.372	100	7.983	1.195	0.542
	10^{-2}	100	2.201	0.568	0.256	100	5.282	0.958	0.417	100	8.437	1.274	0.593
	$5 \cdot 10^{-2}$	100	2.306	0.674	0.348	100	6.566	1.234	0.573	100	12.81	1.804	0.779

Table 8: Comparison of different adversarial attacks on MNIST. ASR means attack success rate (%). N.A. means “not available” due to zero ASR.

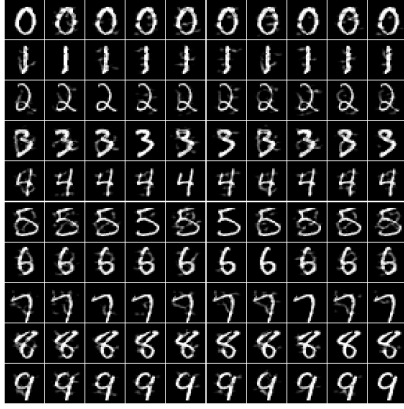
Attack	Best case				Average case				Worst case			
	ASR	L_1	L_2	L_∞	ASR	L_1	L_2	L_∞	ASR	L_1	L_2	L_∞
C&W (L_2)	100	13.93	1.377	0.379	100	22.46	1.972	0.514	99.9	32.3	2.639	0.663
FGM- L_1	99.9	26.56	2.29	0.577	39	53.5	4.186	0.782	0	N.A.	N.A.	N.A.
FGM- L_2	99.4	25.84	2.245	0.574	34.6	39.15	3.284	0.747	0	N.A.	N.A.	N.A.
FGM- L_∞	99.9	83.82	4.002	0.193	42.5	127.2	6.09	0.296	0	N.A.	N.A.	N.A.
I-FGM- L_1	100	18.34	1.605	0.403	100	32.94	2.606	0.591	100	53.02	3.979	0.807
I-FGM- L_2	100	17.6	1.543	0.387	100	30.32	2.41	0.561	99.8	47.8	3.597	0.771
I-FGM- L_∞	100	49.8	2.45	0.147	100	71.39	3.472	0.227	99.9	95.48	4.604	0.348
EAD (EN rule)	100	9.808	1.427	0.452	100	17.4	2.001	0.594	100	25.52	2.582	0.748
EAD (L_1 rule)	100	7.153	1.639	0.593	100	14.11	2.211	0.768	100	22.05	2.747	0.934

Table 9: Comparison of different adversarial attacks on CIFAR10. ASR means attack success rate (%).

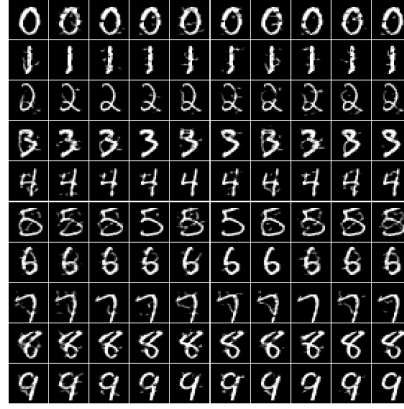
Attack	Best case				Average case				Worst case			
	ASR	L_1	L_2	L_∞	ASR	L_1	L_2	L_∞	ASR	L_1	L_2	L_∞
C&W (L_2)	100	7.167	0.209	0.022	100	13.62	0.392	0.044	99.9	19.17	0.546	0.064
FGM- L_1	99.5	14.76	0.434	0.049	48.8	51.97	1.48	0.152	0.7	157.5	4.345	0.415
FGM- L_2	99.5	14.13	0.421	0.05	42.8	39.5	1.157	0.136	0.7	107.1	3.115	0.369
FGM- L_∞	100	32.74	0.595	0.011	52.3	127.81	2.373	0.047	0.6	246.4	4.554	0.086
I-FGM- L_1	100	7.906	0.232	0.026	100	17.53	0.502	0.055	100	29.73	0.847	0.095
I-FGM- L_2	100	7.587	0.223	0.025	100	17.12	0.489	0.054	100	28.94	0.823	0.092
I-FGM- L_∞	100	17.92	0.35	0.008	100	33.3	0.68	0.018	100	48.3	1.025	0.032
EAD (EN rule)	100	4.014	0.261	0.047	100	8.18	0.502	0.097	100	12.11	0.69	0.147
EAD (L_1 rule)	100	2.597	0.359	0.103	100	6.066	0.613	0.17	100	8.986	0.871	0.27

Table 10: Comparison of different adversarial attacks on ImageNet. ASR means attack success rate (%). N.A. means “not available” due to zero ASR.

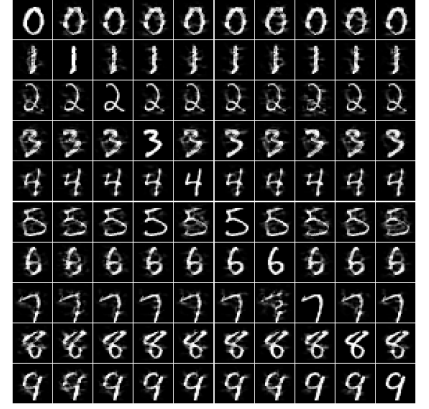
Method	Best case				Average case				Worst case			
	ASR	L_1	L_2	L_∞	ASR	L_1	L_2	L_∞	ASR	L_1	L_2	L_∞
C&W (L_2)	100	157.3	0.511	0.018	100	232.2	0.705	0.03	100	330.3	0.969	0.044
FGM- L_1	9	193.3	0.661	0.025	1	61	0.187	0.007	0	N.A.	N.A.	N.A.
FGM- L_2	12	752.9	2.29	0.087	1	2338	6.823	0.25	0	N.A.	N.A.	N.A.
FGM- L_∞	19	21640	45.76	0.115	3	3655	7.102	0.014	0	N.A.	N.A.	N.A.
I-FGM- L_1	98	292.2	0.89	0.03	77	526.4	1.609	0.054	34	695.5	2.104	0.078
I-FGM- L_2	100	315.4	0.95	0.03	100	774.1	2.358	0.086	96	1326	4.064	0.153
I-FGM- L_∞	100	504.9	1.163	0.004	100	864.2	2.079	0.01	100	1408	3.465	0.019
EAD (EN rule)	100	29.56	1.007	0.128	100	69.47	1.563	0.238	100	160.3	2.3	0.351
EAD (L_1 rule)	100	22.11	1.167	0.195	100	40.9	1.598	0.293	100	100	2.391	0.423



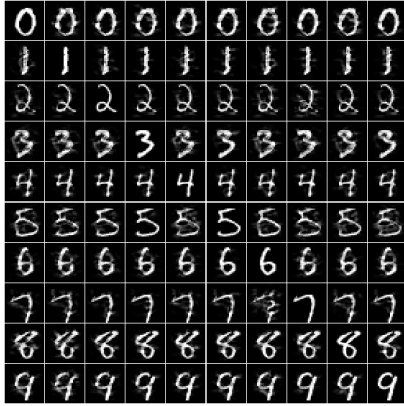
(a) EAD (EN rule)



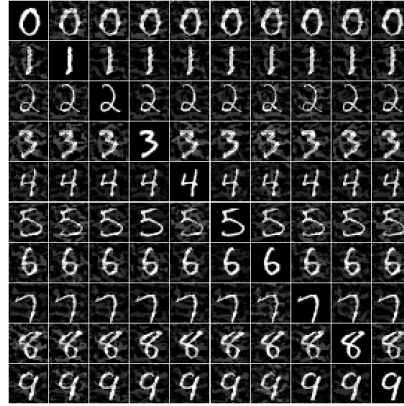
(b) EAD (L_1 rule)



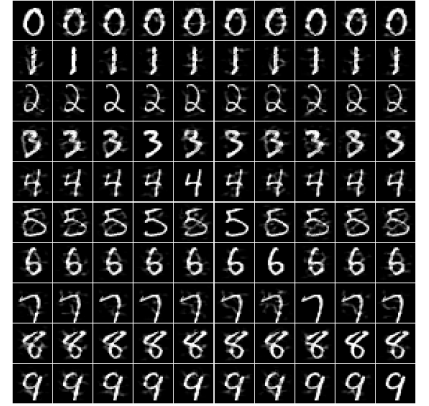
(c) I-FGM- L_1



(d) I-FGM- L_2

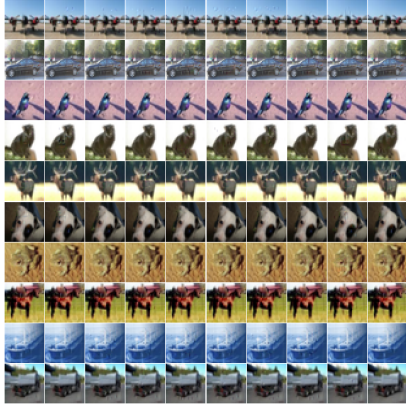


(e) I-FGM- L_∞

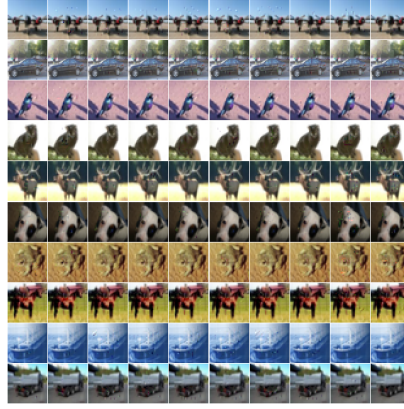


(f) C&W

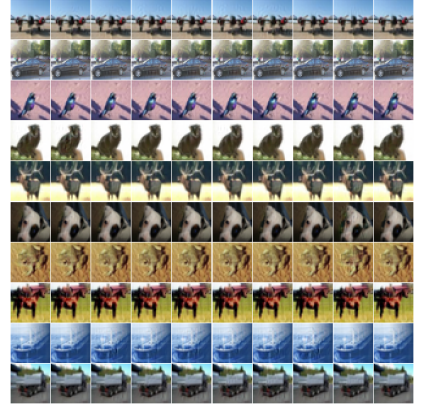
Figure 6: Visual illustration of adversarial examples crafted by different attack methods on MNIST. For each method, the images displayed on the diagonal are the original examples. In each row, the off-diagonal images are the corresponding adversarial examples with columns indexing target labels (from left to right: digits 0 to 9).



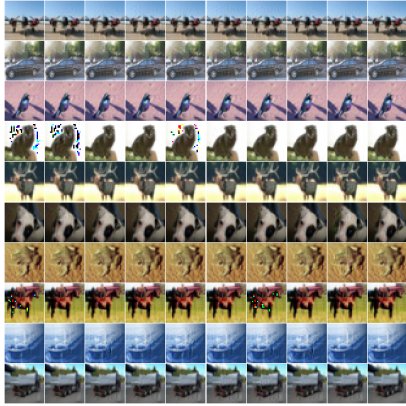
(a) EAD (EN rule)



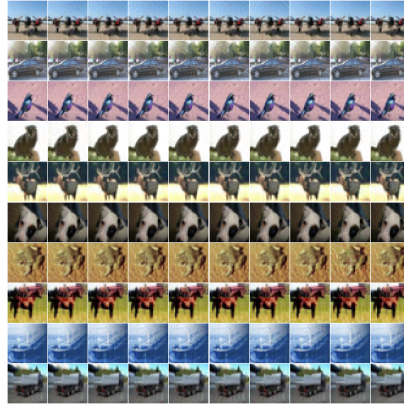
(b) EAD (L_1 rule)



(c) I-FGM- L_1



(d) I-FGM- L_2



(e) I-FGM- L_∞



(f) C&W

Figure 7: Visual illustration of adversarial examples crafted by different attack methods on CIFAR10. For each method, the images displayed on the diagonal are the original examples. In each row, the off-diagonal images are the corresponding adversarial examples with columns indexing target labels.

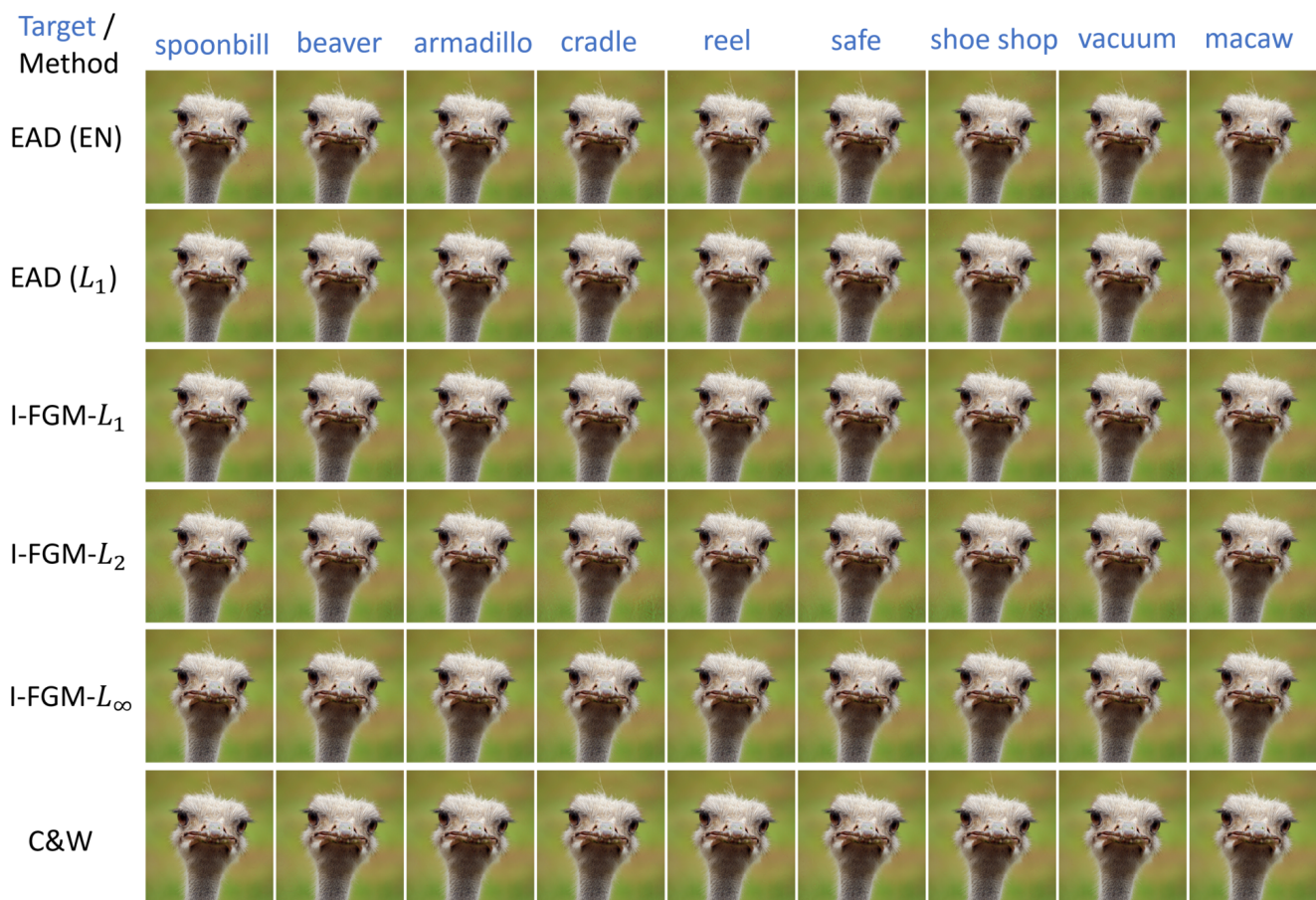


Figure 8: Visual illustration of adversarial examples crafted by different attack methods on ImageNet. The original example is the ostrich image (Figure 1 (a)). Each column represents a targeted class to attack, and each row represents an attack method.

Table 11: Comparison of the C&W method and EAD on attacking defensive distillation with different temperature parameter T on MNIST. ASR means attack success rate (%).

Method	T	Best case				Average case				Worst case			
		ASR	L_1	L_2	L_∞	ASR	L_1	L_2	L_∞	ASR	L_1	L_2	L_∞
C&W (L_2)	1	100	14.02	1.31	0.347	100	23.27	1.938	0.507	99.8	32.96	2.576	0.683
	10	100	16.32	1.514	0.393	100	25.79	2.183	0.539	99.9	36.18	2.882	0.684
	20	100	16.08	1.407	0.336	99.9	26.31	2.111	0.489	99.6	37.59	2.85	0.65
	30	100	16.23	1.409	0.332	99.9	26.09	2.083	0.468	99.7	38.05	2.858	0.629
	40	100	16.16	1.425	0.355	100	27.03	2.164	0.501	100	39.06	2.955	0.667
	50	100	16.48	1.449	0.34	100	26.01	2.111	0.486	99.9	36.74	2.826	0.651
	60	100	16.94	1.506	0.36	100	27.44	2.247	0.512	99.7	38.74	2.998	0.668
	70	100	15.39	1.297	0.297	99.9	25.28	1.961	0.453	99.8	36.58	2.694	0.626
	80	100	15.86	1.315	0.291	100	26.89	2.062	0.46	99.9	38.83	2.857	0.651
	90	100	16.91	1.493	0.357	99.9	27.74	2.256	0.508	99.8	39.77	3.059	0.66
	100	100	16.99	1.525	0.365	99.9	27.95	2.3	0.518	99.8	40.11	3.11	0.67
EAD (EN rule)	1	100	9.672	1.363	0.416	100	17.75	1.954	0.58	100	26.42	2.532	0.762
	10	100	11.79	1.566	0.468	100	20.5	2.224	0.617	100	29.59	2.866	0.768
	20	100	11.54	1.461	0.404	100	20.55	2.133	0.566	100	30.97	2.809	0.719
	30	100	11.82	1.463	0.398	100	20.98	2.134	0.546	100	31.92	2.847	0.701
	40	100	11.58	1.481	0.426	100	21.6	2.226	0.583	100	32.48	2.936	0.739
	50	100	12.11	1.503	0.408	100	21.09	2.161	0.56	99.9	30.52	2.806	0.731
	60	100	12.56	1.559	0.431	100	21.71	2.256	0.588	100	32.47	2.982	0.752
	70	100	11.1	1.353	0.356	100	19.92	2.001	0.518	99.9	29.99	2.655	0.691
	80	100	11.6	1.369	0.347	100	21.08	2.076	0.519	99.7	31.91	2.805	0.712
	90	100	12.57	1.546	0.424	100	22.62	2.312	0.587	99.9	33.38	3.047	0.744
	100	100	12.72	1.575	0.433	100	22.74	2.335	0.596	100	33.82	3.1	0.754
EAD (L_1 rule)	1	100	6.91	1.571	0.562	100	14	2.149	0.758	100	22.41	2.721	0.935
	10	100	8.472	1.806	0.628	100	16.16	2.428	0.798	99.9	25.38	3.061	0.945
	20	100	8.305	1.674	0.556	100	16.16	2.391	0.764	100	25.84	3.031	0.93
	30	100	8.978	1.613	0.51	100	16.48	2.417	0.749	100	25.72	3.124	0.932
	40	100	8.9	1.62	0.536	100	16.74	2.475	0.778	99.9	25.66	3.241	0.947
	50	100	9.319	1.645	0.51	100	17.01	2.401	0.744	100	24.59	3.103	0.939
	60	100	9.628	1.723	0.546	100	17.7	2.477	0.752	100	26.38	3.287	0.944
	70	100	8.419	1.524	0.466	100	16.01	2.193	0.674	100	24.31	2.935	0.892
	80	100	8.698	1.554	0.462	100	17.17	2.283	0.677	100	25.97	3.083	0.904
	90	100	9.219	1.755	0.557	100	18.46	2.529	0.744	99.9	27.9	3.315	0.926
	100	100	9.243	1.801	0.579	100	18.44	2.535	0.759	99.9	28.44	3.351	0.929

Table 12: Comparison of the C&W method and EAD on attacking defensive distillation with different temperature parameter T on CIFAR10. ASR means attack success rate (%).

Method	T	Best case				Average case				Worst case			
		ASR	L_1	L_2	L_∞	ASR	L_1	L_2	L_∞	ASR	L_1	L_2	L_∞
C&W (L_2)	1	100	6.414	0.188	0.02	100	12.46	0.358	0.04	100	17.47	0.498	0.058
	10	100	7.431	0.219	0.024	100	15.48	0.445	0.049	99.9	22.36	0.635	0.073
	20	100	8.712	0.256	0.028	100	18.7	0.534	0.058	100	27.4	0.776	0.087
	30	100	8.688	0.254	0.028	100	19.34	0.554	0.06	99.8	27.67	0.785	0.089
	40	100	8.556	0.251	0.028	100	18.43	0.528	0.058	100	26.89	0.761	0.086
	50	100	8.88	0.26	0.028	100	19.56	0.559	0.06	99.9	29.07	0.822	0.091
	60	100	8.935	0.262	0.029	100	19.43	0.554	0.06	100	28.56	0.809	0.091
	70	100	9.166	0.269	0.03	100	19.99	0.571	0.061	100	29.6	0.838	0.093
	80	100	9.026	0.266	0.029	100	19.93	0.571	0.061	99.5	29.64	0.839	0.092
	90	100	9.466	0.278	0.031	100	21.21	0.606	0.065	100	31.23	0.884	0.099
	100	100	9.943	0.292	0.032	100	21.46	0.614	0.066	99.9	32.54	0.921	0.103
EAD (EN rule)	1	100	3.594	0.236	0.044	100	7.471	0.462	0.09	99.9	10.88	0.638	0.136
	10	100	4.072	0.286	0.052	100	9.669	0.567	0.104	100	14.97	0.782	0.154
	20	100	5.24	0.321	0.056	100	11.79	0.662	0.118	100	17.72	0.932	0.175
	30	100	5.54	0.313	0.051	100	12.33	0.658	0.112	100	18.12	0.94	0.175
	40	100	5.623	0.309	0.05	100	12.02	0.626	0.105	100	18.14	0.915	0.167
	50	100	5.806	0.319	0.05	100	13	0.671	0.109	100	19.46	0.979	0.176
	60	100	6.07	0.319	0.051	100	13.06	0.662	0.109	100	19.5	0.964	0.173
	70	100	6.026	0.33	0.052	100	13.85	0.695	0.111	100	20.06	0.997	0.177
	80	100	5.958	0.327	0.052	100	13.74	0.697	0.111	99.9	20.28	0.999	0.174
	90	100	6.261	0.34	0.054	100	14.07	0.711	0.117	99.9	21.27	1.046	0.189
	100	100	6.499	0.358	0.057	100	15.02	0.756	0.123	100	22.12	1.084	0.192
EAD (L_1 rule)	1	100	2.302	0.328	0.098	100	5.595	0.556	0.154	99.9	8.41	0.776	0.237
	10	100	2.884	0.37	0.101	100	6.857	0.718	0.2	100	10.44	1.037	0.321
	20	100	3.445	0.435	0.118	100	8.943	0.802	0.201	99.9	13.73	1.164	0.322
	30	100	3.372	0.452	0.128	100	8.802	0.796	0.202	100	14.31	1.124	0.304
	40	100	3.234	0.465	0.136	100	8.537	0.809	0.209	100	13.82	1.093	0.297
	50	100	3.402	0.479	0.142	100	8.965	0.848	0.22	100	14.96	1.17	0.317
	60	100	3.319	0.497	0.151	100	8.647	0.863	0.232	99.8	14.46	1.174	0.325
	70	100	3.438	0.506	0.153	100	9.344	0.913	0.239	100	15.06	1.214	0.331
	80	100	3.418	0.5	0.15	100	9.202	0.914	0.242	100	15.14	1.227	0.337
	90	100	3.603	0.519	0.157	100	9.654	0.96	0.258	99.8	15.82	1.287	0.361
	100	100	3.702	0.543	0.161	100	9.839	0.993	0.269	99.8	16.22	1.351	0.379

Table 13: Comparison of attack transferability from the undefended network to the defensively distilled network ($T = 100$) on MNIST with varying transferability parameter κ . ASR means attack success rate (%). N.A. means not “not available” due to zero ASR. There is no κ parameter for I-FGM.

		Best case				Average case				Worst case			
Method	κ	ASR	L_1	L_2	L_∞	ASR	L_1	L_2	L_∞	ASR	L_1	L_2	L_∞
I-FGM- L_1	None	12.2	18.39	1.604	0.418	1.6	19	1.658	0.43	0	N.A.	N.A.	N.A.
I-FGM- L_2	None	9.8	17.77	1.537	0.395	1.3	17.25	1.533	0.408	0	N.A.	N.A.	N.A.
I-FGM- L_∞	None	14.7	46.38	2.311	0.145	1.7	48.3	2.44	0.158	0	N.A.	N.A.	N.A.
C&W (L_2)	0	5.4	11.13	1.103	0.338	1.1	10.16	1.033	0.343	0	N.A.	N.A.	N.A.
	5	16.6	15.58	1.491	0.424	3.4	17.35	1.615	0.46	0	N.A.	N.A.	N.A.
	10	42.2	21.94	2.033	0.525	6.5	21.97	2.001	0.527	0	N.A.	N.A.	N.A.
	15	74.2	27.65	2.491	0.603	22.6	32.54	2.869	0.671	0.4	56.93	4.628	0.843
	20	92.9	29.71	2.665	0.639	44.4	38.34	3.322	0.745	2.4	54.25	4.708	0.91
	25	98.7	30.12	2.719	0.664	62.9	45.41	3.837	0.805	10.9	71.22	5.946	0.972
	30	99.8	31.17	2.829	0.69	78.1	49.63	4.15	0.847	23	85.93	6.923	0.987
	35	100	33.27	3.012	0.727	84.2	55.56	4.583	0.886	30.5	105.9	8.072	0.993
	40	100	36.13	3.255	0.772	87.4	61.25	4.98	0.918	21	125.2	9.09	0.995
	45	100	39.86	3.553	0.818	85.2	67.82	5.43	0.936	7.4	146.9	10.21	0.996
	50	100	44.2	3.892	0.868	80.6	70.87	5.639	0.953	0.5	158.4	10.8	0.996
	55	100	49.37	4.284	0.907	73	76.77	6.034	0.969	0	N.A.	N.A.	N.A.
	60	100	54.97	4.703	0.937	67.9	82.07	6.395	0.976	0	N.A.	N.A.	N.A.
EAD (EN rule)	0	6	8.373	1.197	0.426	0.6	4.876	0.813	0.307	0	N.A.	N.A.	N.A.
	5	18.2	11.45	1.547	0.515	2.5	13.07	1.691	0.549	0	N.A.	N.A.	N.A.
	10	39.5	15.36	1.916	0.59	8.4	16.45	1.989	0.6	0	N.A.	N.A.	N.A.
	15	69.2	19.18	2.263	0.651	19.2	22.74	2.531	0.697	0.4	31.18	3.238	0.846
	20	89.5	21.98	2.519	0.692	37	28.36	2.99	0.778	1.8	39.91	3.951	0.897
	25	98.3	23.92	2.694	0.724	58	34.14	3.445	0.831	7.9	49.12	4.65	0.973
	30	99.9	25.52	2.838	0.748	76.3	40.2	3.909	0.884	23.7	59.9	5.404	0.993
	35	100	27.42	3.009	0.778	87.9	45.62	4.324	0.92	47.4	70.93	6.176	0.999
	40	100	30.23	3.248	0.814	95.2	52.33	4.805	0.945	71.3	83.19	6.981	1
	45	100	33.61	3.526	0.857	98	57.75	5.194	0.965	86.2	98.51	7.904	1
	50	100	37.59	3.843	0.899	98.6	66.22	5.758	0.978	87	115.7	8.851	1
	55	100	42.01	4.193	0.934	94.4	70.66	6.09	0.986	44.2	127	9.487	1
	60	100	46.7	4.562	0.961	90	75.59	6.419	0.992	13.3	140.35	10.3	1
EAD (L_1 rule)	0	6	6.392	1.431	0.628	0.5	6.57	1.565	0.678	0	N.A.	N.A.	N.A.
	5	19	8.914	1.807	0.728	3.2	9.717	1.884	0.738	0	N.A.	N.A.	N.A.
	10	40.6	12.16	2.154	0.773	7.5	13.74	2.27	0.8	0	N.A.	N.A.	N.A.
	15	70.5	15.39	2.481	0.809	19	18.12	2.689	0.865	0.3	23.15	3.024	0.884
	20	90	17.73	2.718	0.83	39.4	24.15	3.182	0.902	1.9	38.22	4.173	0.979
	25	98.6	19.71	2.897	0.851	59.3	30.33	3.652	0.933	7.9	45.74	4.818	0.997
	30	99.8	21.1	3.023	0.862	76.9	37.38	4.191	0.954	22.2	55.54	5.529	1
	35	100	23	3.186	0.882	89.3	41.13	4.468	0.968	46.8	66.76	6.256	1
	40	100	25.86	3.406	0.904	96.3	47.54	4.913	0.979	69.9	80.05	7.064	1
	45	100	29.4	3.665	0.931	97.6	55.16	5.399	0.988	85.8	96.05	7.94	1
	50	100	33.71	3.957	0.95	98.1	62.01	5.856	0.992	85.7	113.6	8.845	1
	55	100	38.09	4.293	0.971	93.6	65.79	6.112	0.995	43.8	126.4	9.519	1
	60	100	42.7	4.66	0.985	89.6	72.49	6.572	0.997	13	141.3	10.36	1

Table 14: Comparison of adversarial training using the C&W attack, EAD (L_1 rule) and EAD (EN rule) on MNIST. ASR means attack success rate.

Attack method	Adversarial training	Best case				Average case				Worst case			
		ASR	L_1	L_2	L_∞	ASR	L_1	L_2	L_∞	ASR	L_1	L_2	L_∞
C&W (L_2)	None	100	13.93	1.377	0.379	100	22.46	1.972	0.514	99.9	32.3	2.639	0.663
	EAD (L_1)	100	15.98	1.704	0.492	100	26.11	2.468	0.643	99.7	36.37	3.229	0.794
	C&W (L_2)	100	14.59	1.693	0.543	100	24.97	2.47	0.684	99.9	36.4	3.28	0.807
	EAD + C&W	100	16.54	1.73	0.502	100	27.32	2.513	0.653	99.8	37.83	3.229	0.795
EAD (L_1)	None	100	7.153	1.639	0.593	100	14.11	2.211	0.768	100	22.05	2.747	0.934
	EAD (L_1)	100	8.795	1.946	0.705	100	17.04	2.653	0.86	99.9	24.94	3.266	0.98
	C&W (L_2)	100	7.657	1.912	0.743	100	15.49	2.628	0.892	100	24.16	3.3	0.986
	EAD + C&W	100	8.936	1.975	0.711	100	16.83	2.66	0.87	99.9	25.55	3.288	0.979
EAD (EN)	None	100	9.808	1.427	0.452	100	17.4	2.001	0.594	100	25.52	2.582	0.748
	EAD (EN)	100	11.13	1.778	0.606	100	19.52	2.476	0.751	99.9	28.15	3.182	0.892
	C&W (L_2)	100	10.38	1.724	0.611	100	18.99	2.453	0.759	100	27.77	3.153	0.891
	EAD + C&W	100	11.14	1.76	0.602	100	20.09	2.5	0.75	100	28.91	3.193	0.882